

Addition of aluminum to solution processed conductive indium tin oxide thin film for an oxide thin film transistor

J. H. Jeon,¹ Y. H. Hwang,¹ B. S. Bae,^{1,a)} H. L. Kwon,² and H. J. Kang²

¹Department of Materials Science and Engineering, KAIST, 373-1, Guseong-dong, Yuseong-gu, Daejeon 305-701, Republic of Korea

²Department of Physics, Chungbuk National University, Cheongju 361-673, Republic of Korea

(Received 23 March 2010; accepted 10 May 2010; published online 28 May 2010)

Aluminum was added to a solution-processed conductive indium tin oxide thin film to be optimized as a channel layer for a thin film transistor (TFT). The conductive crystalline thin film becomes an amorphous semiconductor as the band gap enlarges with increasing Al content. Also, systematic variation in TFT characteristics was observed clearly, displaying transformation to a semiconductor. At the final composition of $(\text{Al}_2\text{O}_3)_{0.3}(\text{In}_2\text{O}_3)_{0.6}(\text{SnO}_2)_{0.1}$, the film channel layer exhibits a high mobility of $13.3 \text{ cm}^2 \text{ V}^{-1} \text{ s}^{-1}$, a high on-to-off ratio of 10^7 and a low subthreshold swing of 1.01 V/dec. © 2010 American Institute of Physics. [doi:10.1063/1.3442482]

Oxide thin film transistors (TFTs) incorporating an oxide active channel layer have been studied for transparent electronics on the strengths of their high mobility, good uniformity, and large band gap. Due to their special conduction mechanism, high carrier mobility can be realized even in the amorphous phase.¹ ZnO, In_2O_3 , and SnO_2 are typical valence compounds with a conduction band derived from spherically symmetric *ns* orbitals with a $(n-1)d^{10}ns^0$ ($n \geq 4$) electronic configuration. The spatial spread of this vacant s-orbital enables direct overlap between neighboring heavy-metal cations. Amorphous oxides with heavy-metal cations, such as indium zinc oxide,² zinc tin oxide (ZTO),³ and indium gallium zinc oxide,¹ have been researched for application as a channel layer of oxide TFTs.

In order to improve the TFT performance, researchers have attempted to control defects by varying the composition of the constituent materials.^{1,5} The defect chemistry of these materials and their derivative compositions strongly affect their optical and electrical properties for use in transparent electronics. Some heavy-metal cations are applicable to oxide TFT owing to their respective advantages: Zn makes it possible not only to obtain an amorphous structure but also to control carrier concentration.³ In and Sn, meanwhile, enhance carrier mobility.⁴ It was reported that the carrier concentration could be effectively controlled through suppression of oxygen vacancy formation by the addition of Ga because Ga has higher bonding energy with oxygen than In or Zn.¹ Also, Al can be employed as an additive in semiconducting oxides, because it has higher bonding energy with oxygen than Ga and also is abundant on earth, resulting in low cost. Al_2O_3 is well known as a good amorphous state stabilizer. Aluminum zinc tin oxide (AZTO) TFTs showed better transfer characteristics without high temperature annealing, while ZTO TFTs fabricated by sputtering required another heat treatment step.⁵ It is thought that the addition of AlO_x makes the optimization of ZTO film easier at room temperature. AZTO TFT also has high temperature stability with various gate structures and passivation.⁶ Likewise, Al addition very sensitively affects the performance of oxide

TFT. However, the effects of AlO_x on the oxide channel have not been clarified yet.

This paper reports on the finding that indium tin oxide (ITO) thin films fabricated by a sol-gel method are transformed from a conductor to a semiconductor by simply adding Al into the composition to enlarge the band gap and transition to an amorphous phase. The optimized composition of a solution-processed aluminum indium tin oxide (AITO) thin film channel layer in a TFT shows high mobility, a high on-to-off current ratio, and a low subthreshold swing, thus making it applicable to the backplane of active matrix organic light emitting diode and active matrix liquid crystal displays.

The ITO solutions were prepared by dissolving precursors with a molar ratio 90% of indium acetate and 10% of tin chloride in 2-methoxyethanol. For the addition of Al to the ITO solutions, we applied a molar ratio of 20%, 40%, and 60% of aluminum acetylacetonate with an indium precursor while maintaining the tin precursor at 10%. In order to form stable solutions, ethylenediamine is added as a chelating agent. Each solution was stirred at room temperature for 2 h becoming transparent and homogeneous. After sufficient reaction, the solutions were filtered through a 0.22 μm syringe filter. Because 75% of weight loss of the precursors was decomposed at a temperature of around 300 °C, as determined by thermogravimetric analysis, the solutions were annealed at 500 °C in air for 2 h after spin-coating on a $\text{SiO}_2/\text{p}^+\text{-Si}$ substrate at a speed of 4000 rpm for 30 s. The film composition was distributed uniformly, according to a composition analysis using x-ray photoelectron spectroscopy (XPS). Finally, four different thin film compositions, $(\text{Al}_2\text{O}_3)_x(\text{In}_2\text{O}_3)_{0.9-x}(\text{SnO}_2)_{0.1}$ [$x=0, 0.2, 0.3, 0.45$] were prepared. The thickness of the annealed thin films was approximately 10 nm. The chemical state and the band gap of the thin films were investigated by utilizing XPS and reflection electron energy loss spectroscopy (REELS). Both of the spectra were obtained by using VG ESCALAB 210 equipment. XPS binding energies were referenced to the C 1s peak of hydrocarbon contamination at 285 eV and REELS were measured with a primary electron energy of 1.5 keV for excitation. To fabricate and characterize the TFT, 100 nm thick Al electrodes for source-drain contacts were deposited

^{a)}Author to whom correspondence should be addressed. Electronic mail: bsbae@kaist.ac.kr.

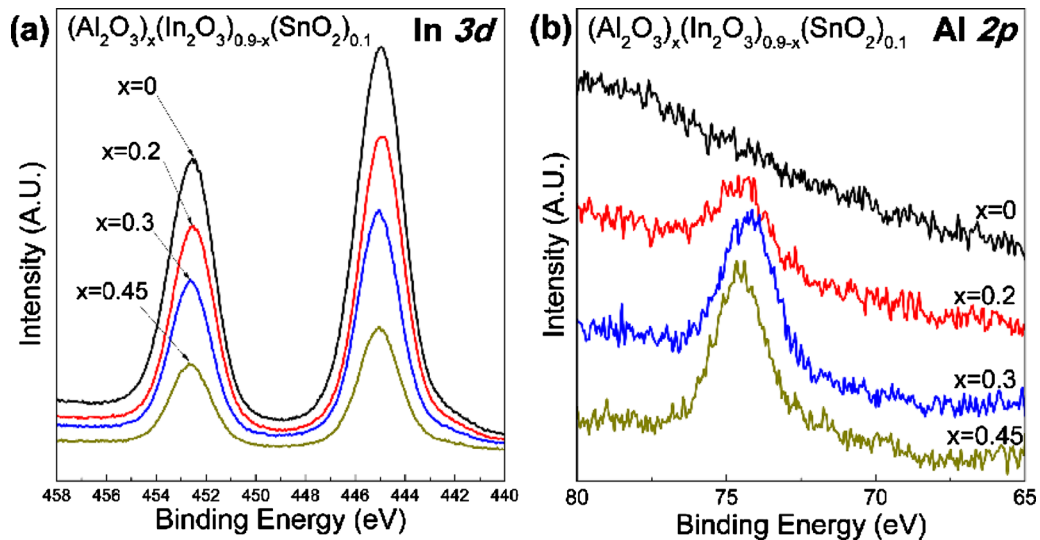


FIG. 1. (Color online) In 3d (a) and Al 2p (b) core level x-ray photoelectron spectra for $(\text{Al}_2\text{O}_3)_x(\text{In}_2\text{O}_3)_{0.9-x}(\text{SnO}_2)_{0.1}$ thin films.

on an oxide film on a $\text{SiO}_2/\text{p}^+\text{-Si}$ structure by e-beam evaporation so as to form an inverted gated device structure (Al/Oxide thin film/ $\text{SiO}_2/\text{p}^+\text{-Si}$). The TFT characteristics of the devices were analyzed using a HP 4145B semiconductor parameter analyzer in a dark room at ambient conditions.

Figure 1 shows the XPS results of the In 3d and Al 2p states of the thin films depending on the composition of the films. The binding energies of In $3d_{5/2}$ and In $3d_{3/2}$ peaks with oxygen were measured at 445.0 eV and 452.6 eV respectively,^{7,8} as indicated in Fig. 1(a). Both peaks decreased with increasing Al content in the thin films. In Fig. 1(b), the Al 2p core-level located at 74.5 eV is observed for Al added thin films and is enhanced with increasing Al content.^{9,10} Also, we investigated x-ray diffraction (results not presented in this paper) to confirm the crystallinity of the thin films. It was clearly observed that the diffraction peak in the thin film is diminished with Al addition. Thus, it is found that the addition of Al suppressed the indium oxide matrix transitioning to an amorphous phase.¹¹

To investigate the electronic band gap, E_g , of the thin films, a REELS analysis was performed. The electronic

structure near E_g by fitting two lines to the REELS spectrum.¹² One line is fit to the onset of a loss-signal spectrum at a point where the slope has a maximum negative value. The other is fit to the background level. The loss energy value of the intersection of these lines gives E_g . As represented in Fig. 2(a), E_g increases from 3.3 to 4.0 eV as Al is increasingly incorporated in the ITO composition. Also, the optical band gap, E_{opt} , was obtained from the optical absorption spectra of the thin films. From the plot of $(\alpha h\nu)^{1/2}$ versus $h\nu$ shown in Fig. 2(b), E_{opt} obtained from the intersection of extrapolation of a linear plot with the axis, increases from 3.33 to 3.99 eV with increasing Al content in the thin films. This is almost identical with E_g . Thus, it is confirmed that the addition of Al to the ITO composition enlarges the band gap, transforming a conductor to a semiconductor.

Figure 3 shows the transfer curves of the TFTs with various oxide thin film channel layer compositions. The transfer curve for ITO thin films without addition of Al shows a monotonous increase in current with the gate volt-

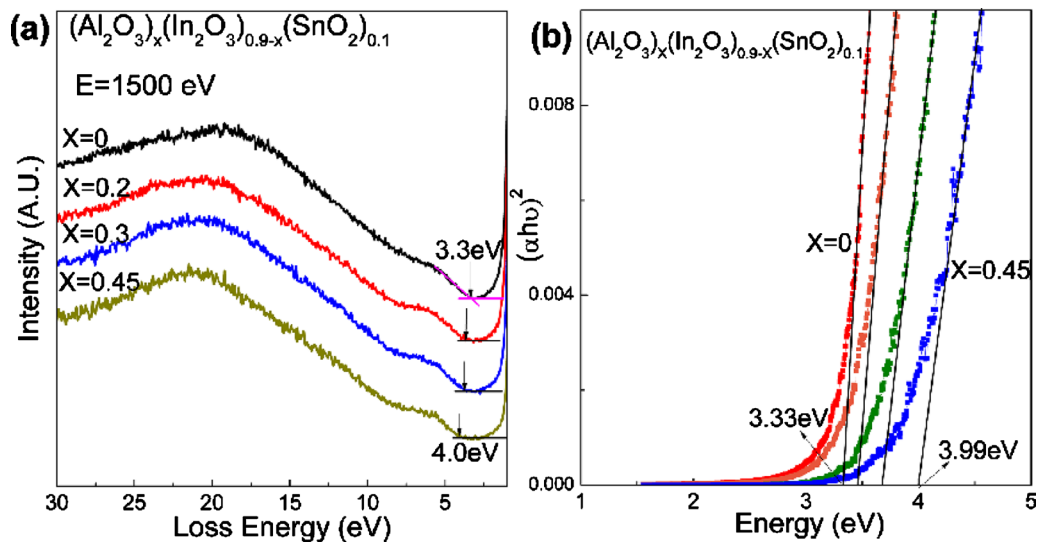


FIG. 2. (Color online) (a) Reflection electron energy loss spectra for $(\text{Al}_2\text{O}_3)_x(\text{In}_2\text{O}_3)_{0.9-x}(\text{SnO}_2)_{0.1}$ thin films with the primary electron energy of 1500 eV. (b) The optical band gap of $(\text{Al}_2\text{O}_3)_x(\text{In}_2\text{O}_3)_{0.9-x}(\text{SnO}_2)_{0.1}$ thin films calculated from the optical absorption spectra of at 200–800 nm.

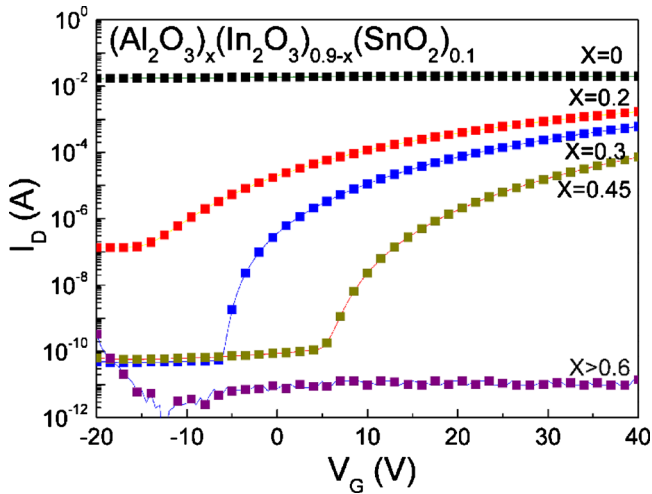


FIG. 3. (Color online) Transfer curves for $(\text{Al}_2\text{O}_3)_x(\text{In}_2\text{O}_3)_{0.9-x}(\text{SnO}_2)_{0.1}$ TFTs having the following structures: $\text{Si}/\text{SiO}_2(100 \text{ nm})/(\text{Al}_2\text{O}_3)_x(\text{In}_2\text{O}_3)_{0.9-x}(\text{SnO}_2)_{0.1}(\sim 10 \text{ nm})/\text{Al}(100 \text{ nm})$, $L=220 \mu\text{m}$, $W=1000 \mu\text{m}$.

age, and indication of conductorlike behavior. The static resistivity of the ITO thin film was measured as $2.5 \times 10^{-4} \Omega \text{ cm}$ by 4-point probe sensing and it abruptly increased even with a very small addition of Al content. With the addition of Al into the ITO composition, the current level is lowered showing the off-state for the device to become a transistor. As the Al content in the channel layer increases further, the negative threshold voltage shifts toward zero and the current level difference between the on and off states becomes greater, clearly displaying a semiconducting property. The TFT for $x=0.3$ composition channel shows the best overall device performance. For this sample, the carrier mobility is around $13.3 \text{ cm}^2 \text{ V}^{-1} \text{ s}^{-1}$, whereas the on-to-off current ratio is close to 10^7 . The off-current remains lower than 10^{-10} A and the subthreshold swing is 1.01 V/decade . As the Al content is increased further, the on-state current is reduced, becoming flat for the $x=0.6$ composition. Thus, the aluminum oxide dominant matrix composition presents an insulatorlike property. With overly high Al contents the film matrix to become aluminum oxide dominant.

This systematic variation in the transfer curve with the addition of Al to the ITO composition was manifested by the transformation from a conductor to a semiconductor, as already shown in the variation in the band gap of the thin films. The increased band gap with increasing Al in the composition results in the obstruction of carrier transfer as well as lower carrier concentration. The replacement of In with Al in the composition suppresses overlapping between adjacent metal cations since Al is a light-metal cation with a small ns orbital. The reduction in orbital overlapping restrains the electronic path for moving carriers. In addition, Al has basically higher chemical bonding energy with oxygen than other metal cations such as In or Sn. Thus, the addition of Al produces fewer oxygen vacancies, resulting in low carrier concentration. E_g due to the formation of AlO_x in AITO channel meanwhile becomes larger. The conduction in the semiconductor occurs due to carriers that are created via electron-hole pair generation, where the electron from the valence band is excited to the conduction band over E_g . The larger E_g requires higher energy for the electron-hole pair

generation, and it is also necessary to apply higher voltages to move the carrier. Accordingly, V_{th} shifts and the mobility decreases at the AITO channel with higher Al contents. Finally, we can obtain an AITO channel with a semiconducting property for an oxide TFT from conductive ITO by controlling the defects and E_g via Al addition.

In summary, we fabricated an AITO channel layer for application in an oxide TFT by simply changing the composition with Al addition to a solution-processed conductive ITO thin film. With increasing Al content, the core level spectra of Al $2p$ and In $3d$ by XPS represents an increase in aluminum oxide in the AITO thin film. The band gaps by REELS were measured as 3.3 eV for a $x=0$ composition of $(\text{Al}_2\text{O}_3)_x(\text{In}_2\text{O}_3)_{0.9-x}(\text{SnO}_2)_{0.1}$ thin film and increases to 4.0 eV for $x=0.45$ composition. This dependence by Al addition to the ITO thin film was also manifested in the TFT characteristics. The electrical behavior transformed from conducting to semiconducting with increase in the Al composition, resulting in lower off-current and a positive shift of the threshold voltage. We speculated that Al addition could contribute to the nonguaranteed electronic path due to insufficient overlapping between adjacent cations because of the small ns orbital of Al and lowered carrier concentration due to a larger band gap formed by aluminum oxide in the ITO thin film. Using this concept, we fabricated a semiconducting channel layer for an oxide TFT having high carrier mobility of $13.3 \text{ cm}^2 \text{ V}^{-1} \text{ s}^{-1}$, a high on-to-off current ratio of 10^7 , and a low subthreshold swing of 1.01 V/dec . by tuning the Al composition of the AITO channel with a $x=0.3$ composition. This study sheds light on how Al affects the chemical and electronic structure of Al-added oxide thin films for transparent electronics.

This research was supported by Basic Science Research Program through the National Research Foundation of Korea (NRF) funded by the Ministry of Education, Science and Technology (Grant No. CAFDC-20100009898) and by the Ministry of Knowledge Economy (MKE) and Korea Institute for Advancement in Technology (KIAT) through the Workforce Development Program in Strategic Technology.

¹K. Nomura, H. Ohta, A. Takagi, T. Kamiya, M. Hirano, and H. Hosono, *Nature (London)* **432**, 488 (2004).

²D. Lee, Y. Chang, G. S. Herman, and C. Chang, *Adv. Mater.* **19**, 843 (2007).

³H. Q. Chiang, J. F. Wager, R. L. Hoffman, J. Jeon, and D. A. Keszler, *Appl. Phys. Lett.* **86**, 013503 (2005).

⁴M. S. Grover, P. A. Hersh, H. Q. Chiang, E. S. Kettenring, J. F. Wager, and D. A. Keszler, *J. Phys. D: Appl. Phys.* **40**, 1335 (2007).

⁵D. H. Cho, S. Yang, C. Byun, J. Shin, M. K. Ryu, S. H. Ko Park, C. S. Hwang, S. M. Chung, W. S. Cheong, S. M. Yoon, and H. Y. Chu, *Appl. Phys. Lett.* **93**, 142111 (2008).

⁶J. K. Jeong, S. H. Yang, D. H. Cho, S. H. Ko Park, C. S. Hwang, and K. I. Cho, *Appl. Phys. Lett.* **95**, 123505 (2009).

⁷K. P. Kim, A. M. Hussain, D. K. Hwang, S. H. Woo, H. K. Lyu, S. H. Baek, Y. Jang, and J. H. Kim, *Jpn. J. Appl. Phys., Part 2* **48**, 021601 (2009).

⁸T. F. Stoica, M. Gartner, T. Stoica, M. Losurdo, V. S. Teodorescu, M. G. Blanchin, and M. Zaharescu, *J. Optoelectron. Adv. Mater.* **7**, 2353 (2005).

⁹S. Wannaparhun, S. Seal, and V. Dei, *Appl. Surf. Sci.* **185**, 183 (2002).

¹⁰M. Nguefack, A. F. Popa, S. Rossignol, and C. Kappenstein, *Phys. Chem. Chem. Phys.* **5**, 4279 (2003).

¹¹Y. H. Hwang, J. H. Jeon, S. J. Seo, and B. S. Bae, *Electrochem. Solid-State Lett.* **12**, H336 (2009).

¹²H. Jin, S. K. Oh, H. J. Kang, and M. H. Cho, *Appl. Phys. Lett.* **89**, 122901 (2006).